Int J Thermophys (2009) 30:1227–1233
DOI 10.1007/s10765-009-0623-1

Thermal Characterization of Nanofluids with Different Solvents

J. L. Jiménez-Pérez · A. Cruz-Orea · J. F. Sánchez-Ramírez · F. Sánchez-Sinencio · L. Martínez-Pérez · G. A. López Muñoz

Received: 14 October 2008 / Accepted: 10 July 2009 / Published online: 19 August 2009

Abstract Thermal lens spectrometry (TLS) and photopyroelectric (PPE) techniques were used to obtain the thermal diffusivity and effusivity of different nanofluid samples. The thermal effusivity of these samples was obtained by the PPE technique in a front detection configuration. In the case of the determination of the thermal diffusivity, TLS was used for the different solvents in the presence of gold nanoparticles (nanofluids). In this technique, an Ar^+ laser and intensity stabilized He–Ne laser were used as the heating source and probe beam, respectively. The experimental results showed that thermal diffusivity values of the studied solvents (water, ethanol, and ethylene glycol) were enhanced by the presence of gold nanoparticles. Comparisons with literature values show good agreement with pure solvents. These techniques are applicable for all kind of liquid samples, including semitransparent ones.

Keywords Nanoparticles · Thermal lens · Thermal properties of small particles · Transmission electron microscope

1 Introduction

In recent years, photothermal techniques have experienced great expansion; they are used in a wide range of scientific disciplines to carry out studies of diverse properties of

J. L. Jiménez-Pérez · L. Martínez-Pérez · G. A. López Muñoz
UPIITA-IPN, Av. IPN. 2580, Col. Barrio La Laguna, Ticomán, Del. Gustavo A. Madero, C.P. 07340 Mexico, DF, Mexico

A. Cruz-Orea (✉) · F. Sánchez-Sinencio
Physics Department, CINVESTAV-IPN, A.P. 14-740, 07360 Mexico, DF, Mexico
e-mail: orea@fis.cinvestav.mx

J. F. Sánchez-Ramírez
CICATA-IPN, Legaria 694, Col. Irrigación, 11500 Mexico, DF, Mexico

condensed matter including optical, transport, and thermal properties [1]. Considering the thermal properties, the photopyroelectric (PPE) and thermal lens (TL) techniques have been employed for thermal characterization of several samples by measuring their thermal effusivity and diffusivity [2]. For example, thermal lens spectrometry (TLS) has been used recently for thermal characterization of metal nanoparticles. Metallic nanoparticles are of great importance because of their unique electronic, magnetic, and optical properties [3,4]. A comprehensive understanding of the electron dynamics and relaxation processes in these systems is required because of their fast optical response, which is very important for many potential applications such as optical switching and electronic devices [5,6]. Moreover, a better understanding of some other properties such as electrical and thermal conductivity and superconductivity of metallic nanoparticles could be achieved by studying the relaxation dynamics.

The TL effect, for example, is one of the thermo-optical methods usually employed for measurements of the thermal diffusivity. A TL occurs when energy absorbed from a Gaussian beam produces local heating within the absorbing medium around the beam axis. In such experiments, the sample is exposed to a laser beam which has a Gaussian profile and it causes excitation of the molecules along the beam path. Thermal relaxation of the excited molecules dissipates heat into the surroundings, thereby creating a temperature distribution that produces a refractive index gradient normal to the beam axis within the medium. This acts as a diverging lens and is called a TL [7]. On the other hand, we obtained the thermal effusivity by the PPE technique. In this technique, the temperature variation of a sample exposed to modulated radiation is measured with a pyroelectric sensor. In the last few years, this method has been applied to the study of optical and thermal properties of materials. There are two practical detection configurations proposed for PPE calorimetry, i.e., the standard (back) and inverse (front) configurations [8,9], and all four static (specific heat (c) and thermal conductivity (k)) and dynamic (thermal diffusivity (α) and thermal effusivity (e)) thermal parameters can be measured by combining various specific cases [10–12]. In this article, we applied a PPE front configuration scheme for measuring the thermal effusivity of nanofluids.

Using PPE and TL techniques, we have determined the thermal effusivity and thermal diffusivity of three different solvents [ethanol, water, and ethylene glycol (EG)] with gold nanoparticles. This process corresponds to the heat transfer from the metal particles to the environment; this energy dissipation from a metallic nanoparticle and its environment is not yet completely understood.

2 Photothermal Measurements

The thermal effusivities in the experimental configuration are ($e_i = \sqrt{(k_i \rho_i c_i)}$), where i = s, g, p (sample, gas, and pyroelectric, respectively); ρ_i is the density of the i-th medium and e_s for the samples was obtained by using the PPE technique in a front detection configuration. The experimental setup used for these measurements is shown in Ref. [12]. A He–Ne laser beam, whose light was modulated by an acousto-optical modulator, impinged on the pyroelectric transducer. On the other side of this transducer was placed the liquid sample, which had good thermal contact with the pyroelectric

transducer. All the PPE measurements were normalized to the empty PPE cell to avoid the frequency response of the pyroelectric detector. Using the theory proposed by Mandelis and Zver [10,11] and the approximation of Caerels and Glorieux [12], the thermal diffusivity was obtained from the best fit of the following equation to the experimental data, by taking b as a fitting parameter:

$$\theta(\omega) = \frac{E\left(\beta + g\sigma_{\mathrm{p}}\right)}{\sigma_{\mathrm{p}}^2 L_{\mathrm{p}}} \times \left[\frac{\left(1 - \mathrm{e}_{\mathrm{p}}^{\sigma} L_{\mathrm{p}} \left[(1-b)(1-h)\,\mathrm{e}^{-\sigma_{\mathrm{s}} L_{\mathrm{s}}} + (1+b)(1+h)\,\mathrm{e}^{\sigma_{\mathrm{s}} L_{\mathrm{s}}}\right] + \left(\mathrm{e}_{\mathrm{p}}^{\sigma} L_{\mathrm{p}} - 1\right)[1+b](1-h)\,\mathrm{e}^{-\sigma_{\mathrm{s}} L_{\mathrm{s}}} + (1-b)(1+h)\,\mathrm{e}^{\sigma_{\mathrm{s}} L_{\mathrm{s}}}\right)}{\left[(1+b)(1-h)\,\mathrm{e}^{-\sigma_{\mathrm{s}} L_{\mathrm{s}}} + (1-b)(1+h)\,\mathrm{e}^{\sigma_{\mathrm{s}} L_{\mathrm{s}}}\right](g-1)\,\mathrm{e}_{\mathrm{p}}^{-\sigma} L_{\mathrm{p}} + \left[(1-b)(1-h)\,\mathrm{e}^{\sigma_{\mathrm{s}} L_{\mathrm{s}}} + (1+b)(1+h)\,\mathrm{e}^{\sigma_{\mathrm{s}} L_{\mathrm{s}}}\right](1+g)\,\mathrm{e}_{\mathrm{p}}^{\sigma} L_{\mathrm{p}}} \right] \tag{1}$$

with

$$E = \frac{\beta I_0}{2K_{\mathrm{p}}\left(\beta^2 - \sigma_{\mathrm{p}}^2\right)}, \quad \sigma_j = (1+i)\frac{1}{\mu_j} = (1+i)\sqrt{\frac{\pi f}{\alpha_j}}$$
$$g = \frac{e_{\mathrm{g}}}{e_{\mathrm{p}}}, \quad b = \frac{e_{\mathrm{s}}}{e_{\mathrm{p}}}, \quad h = \frac{e_{\mathrm{g}}}{e_{\mathrm{s}}},$$

where β is the optical absorption coefficient of the pyroelectric detector. In order to simplify Eq. 1 to obtain the sample thermal effusivity, we chose a light modulation frequency (f) range where the sample is considered as thermally thick ($(\pi f/\alpha)^{1/2} L_{\mathrm{s}} \gg 1$, where L_{s} is the sample thickness).

On the other hand using TL spectrometry, the thermal diffusivity of these samples was obtained. The TL effect of such nanofluids was based on laser-induced heating and time-resolved monitoring of the thermal effects. A schematic diagram of the TL experimental setup is shown in Ref. [13]. From aberrant model theory, the time evolution of the probe beam intensity $I(t)$ at the detector is [7]

$$I(t) = I(0)\left[1 - \frac{\theta}{2}\tan^{-1}\left(\frac{2mV}{\left[(1+2m)^2 + V^2\right]\frac{t_{\mathrm{c}}}{2t} + 1 + 2m + V^2}\right)\right]^2 \tag{2}$$

where

$$m = \left(\frac{\omega_{1\mathrm{p}}}{\omega_{\mathrm{e}}}\right)^2; \quad V = \frac{Z_1}{Z_{\mathrm{c}}}; \quad \theta = -\frac{P_{\mathrm{e}} A_{\mathrm{e}} l_0}{k\lambda_{\mathrm{p}}}\left(\frac{\mathrm{d}n}{\mathrm{d}T}\right)_{\mathrm{p}}$$

and

$$t_c = \frac{\omega_e^2}{4\alpha} \tag{3}$$

Here $I(0)$ is the initial intensity when t or θ is zero, P_e is the excitation beam power (40 mW), A_e is the absorption coefficient (m^{-1}), l_0 is the sample thickness, λ_p is the probe beam wavelength (630 nm), dn/dT is the refractive index change of the sample with temperature (K^{-1}), $Z_c = \pi\omega_{op}^2/\lambda$ is the confocal distance (m), Z_1 is the distance of the probe beam waist to the sample, $\alpha = \kappa/(\rho c)$ is the thermal diffusivity ($m^2 \cdot s^{-1}$) of the sample, where κ, ρ, and c are the thermal conductivity ($J \cdot s^{-1} \cdot m^{-1} \cdot K^{-1}$), density ($kg \cdot m^{-3}$) and the specific heat of the sample ($J \cdot kg^{-1} \cdot K^{-1}$), respectively. Also, t_c is the characteristic thermal time constant (s). ω_e, Z_c, ω_{1p}, and ω_{op} can be obtained from the spot size measurements [7], and θ and t_c can be determined by fitting Eq. 2 to the measured time-resolved intensity signal, $I(t)$. The thermal diffusivity α can be determined from t_c in Eq. 3.

3 Experimental

Fluids containing gold (Au) nanoparticles were prepared by reduction of gold ions in the presence of poly(*N*-vinyl-2-pirrolidone) (PVP) using ascorbic acid (AA) as a reducing agent with some modifications [14]. The fluids were then diluted to a Au content of 0.033 mmol in 50 ml of water (or ethanol or EG) and were placed in a quartz cuvette of 1cm thickness for the optical and thermal measurements.

A Shimadzu UV–Vis 3101PC double beam spectrophotometer was used to record the absorption spectra of the fluids. Particle sizes and size distribution were evaluated by TEM, using a JEOL-JEM200 microscope. For TEM observations, a drop of colloidal solution was spread on a carbon-coated copper micro-grid and dried subsequently in vacuum. Gold particles with an average size of 13.9 nm were obtained.

4 Results and Discussion

Thermal lens measurements were made with gold nanoparticles in different solvents for the determination of thermal diffusivity values. An absorption peak around 528 nm was revealed in these fluids, which is assigned to the surface plasmon resonance (SPR). From the TEM image the corresponding average of the Au particle size is 13.9 nm. The TL signal measurements were carried out for 0.033 mmol gold nanoparticle content in 50 ml of water (or ethanol or EG). The dependence of the TL signal on time for gold nanoparticles in water, ethanol, and EG systems was studied, and the results showed that the TL signal intensity varies exponentially with time. Figure 1 shows the variation of the intensity of the TL signal: the symbols (o) represent the experimental points and the solid line corresponds to the best fit of Eq. 1 to the experimental data leaving θ and t_c as adjustable parameters. From this fit the values of $\theta = (2.75 \pm 0.01)$ and $t_c = (4.2 \pm 0.08)$ ms were obtained, corresponding to a thermal diffusivity $\alpha = (9.5 \pm 0.2) \times 10^{-8} m^2 \cdot s^{-1}$ for gold nanoparticles with

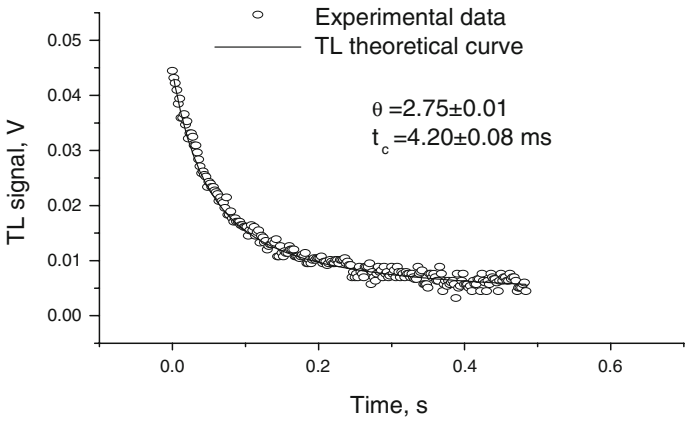

Fig. 1 Time evolution of the TL signal for sample of gold nanoparticles + ethanol

ethanol. Compared with a reported value of the thermal diffusivity for pure ethanol ($\alpha = 8.78 \times 10^{-8} \mathrm{m}^2 \cdot \mathrm{s}^{-1}$), it is possible to see an enhancement of 8.4 %. From the TL signal in the other samples, thermal diffusivity values of $(15.3 \pm 0.5) \times 10^{-8} \mathrm{m}^2 \cdot \mathrm{s}^{-1}$ and $(10.5 \pm 0.3) \times 10^{-8} \mathrm{m}^2 \cdot \mathrm{s}^{-1}$ were obtained for gold nanoparticles in water and EG as solvents, respectively. These results show an enhancement of 7 % and 0.7 % in the thermal diffusivities for water and EG, respectively. Table 1 summarizes the thermal diffusivity values obtained from the fit of Eq. 2 to experimental data and the corresponding values for pure solvents [15]. A possible explanation of this enhancement in the thermal diffusivity for the different solutions with Au nanoparticles could be due to the electrostatic interaction between the cationic solution and the negatively charged Au nanoparticles. Then laser excitation would lead to the generation of hot electrons which are rapidly thermalized by electron-phonon scattering [16]. The energy deposited into the phonon modes is subsequently transferred to the surrounding medium. On the other hand, the thermal effusivity was obtained by fitting Eq. 1, in the case of thermally thick samples ($(\pi f/\alpha)^{1/2} l \gg 1$), to the normalized amplitude and phase experimental data. Figure 2 shows the best fit of Eq. 1 to the (a) amplitude and (b) phase experimental data, taking b as a fitting parameter. It is possible to see that the thermal effusivity had a behavior in opposition to the results for the thermal diffusivity, which is due to the fact that both physical properties are inversely proportional ($e = k/\sqrt{\alpha}$). Also, from the measured thermal diffusivity and thermal effusivity, the thermal conductivity and heat capacity per volume unit of each sample were obtained; these values are also displayed in Table 1, and they are close to the literature values reported for pure solvents [15].

5 Conclusions

Using PPE and TL techniques, the thermal effusivity and thermal diffusivity of gold nanoparticles were obtained, at a fixed concentration in different solvents such as water, EG, and ethanol. The results show that the thermal diffusivity of the different

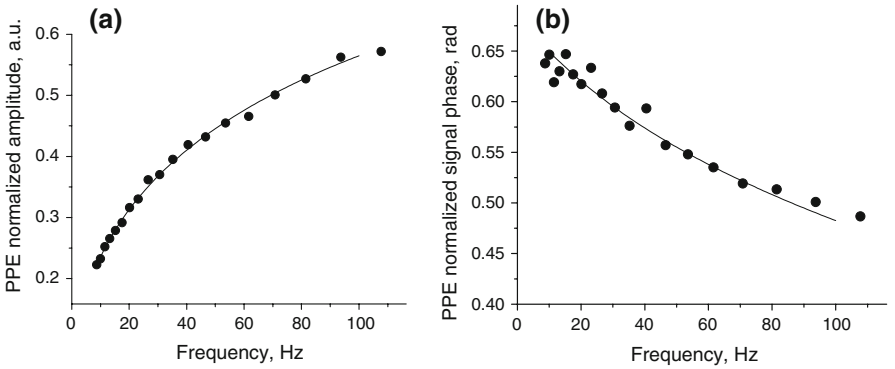

Fig. 2 PPE (**a**) normalized amplitude and (**b**) phase for sample of gold nanoparticles + ethanol as a function of the light modulation frequency. *Dots* are the experimental data and *solid line* is the best fit to Eq. 1

Table 1 Experimental α and e and calculated k and ρc for solvents with gold nanoparticles and α and e values of pure solvents from the literature [15]

Solution	$e \times 10^4$ ($\mathrm{W{\cdot}s^{1/2}{\cdot}m^{-2}{\cdot}K^{-1}}$)	α ($\mathrm{10^{-8}m^2{\cdot}s^{-1}}$)	Pure solvent α ($\mathrm{10^{-8}m^2{\cdot}s^{-1}}$) literature	Pure solvent $e \times 10^4$ ($\mathrm{W{\cdot}s^{1/2}{\cdot}m^{-2}{\cdot}K^{-1}}$) literature	Thermal conductivity k ($\mathrm{W{\cdot}m^{-1}{\cdot}K^{-1}}$)	Heat capacity per volume unit $\rho c \times 10^6$ ($\mathrm{J{\cdot}m^{-3}{\cdot}K^{-1}}$)
AU/H_2O	0.142 ± 0.002	15.3 ± 0.5	14.08 ± 0.09(H_2O)	0.157 (H_2O)	0.56 ± 0.02	3.62 ± 0.01
AU/EG	0.080 ± 0.001	10.5 ± 0.3	10.4 (EG)	0.081 (EG)	0.25 ± 0.011	2.5 ± 0.01
AU/ethanol	0.051 ± 001	9.5 ± 0.2	8.78 (ethanol)	0.057 (ethanol)	0.157 ± 0.005	1.67 ± 0.001

solvents, mixed with gold nanoparticles, increases when compared with the pure solvents, enhancing this thermal parameter in the solution. This study is important for industrial applications where the efficiency of heat transfer is of fundamental significance.

Acknowledgments We would like to thank Conacyt, and SIP-IPN, México for their partial financial support. The authors are also grateful to Ing. E. Ayala Maycotte, Ing. A. B. Soto, Ing. D. Jacinto Méndez, and Ing. M. Guerrero of the Physics Department, CINVESTAV-IPN for their technical assistance.

References

1. P. Keblinski, J.A. Eastman, D.G. Cahill, Mater. Today **8**, 36 (2005)
2. D. Dadariat, H. Visser, D. Bicanic, Meas. Sci. Technol. **6**, 1215 (1995)
3. U. Kreibig, M. Vollmer, *Optical Properties of Metal Clusters* (Springer, Berlin, 1995)
4. P. Mulvaney, Langmuir **12**, 788 (1996)
5. G. Shon, U. Simon, Colloid Polym. Sci. **12**, 202 (1995)
6. A.S. Edelstein, R.C. Cammarata, *Nanoparticles Synthesis Properties and Application* (Institute of Physics Pub, Bristol, 1996)
7. J. Shen, R.D. Lowe, R.D. Snook, Chem. Phys. **165**, 385 (1992)
8. D. Dadarlat, C. Neamtu, E. Surducan, A. Hardj Sahraoui, S. Longuemart, D. Bicamic, Instrum. Sci. Technol. **30**, 387 (2002)

9. S. Longuemart, A. Garcia Quiroz, D. Dadarlat, A. Hardj Sahraoui, J. Marc Busine, E. Correa da Silva, A.M. Mansanares, X. Filipand, C. Neamtu, Instrum. Sci. Technol. **30**, 157 (2002)
10. A. Mandelis, Chem. Phys. Lett. **108**, 388 (1984)
11. A. Mandelis, M. Zver, J. Appl. Phys. **57**, 4421 (1985)
12. J. Caerels, C. Glorieux, J. Thoen, Instrum. Sci. Technol. **69**, 2452 (1998)
13. J.L. Jiménez Pérez, J.F. Sánchez Ramírez, R. Gutiérrez Fuentes, A. Cruz Orea, J.L. Herrera Pérez, Braz. J. Phys. **36**, 1025 (2006)
14. J. Park, V. Privman, E. Matijevic, J. Phys. Chem. B **105**, 11630 (2001)
15. R.C. Weast, *CRC Handbook of Chemistry and Physics*, 67th edn. (CRC Press, Boca Raton, FL, 1986–1987)
16. C.V. Bindhu, S.S. Harilal, V.P.N. Nampoori, C.P.G. Vallabhan, Mod. Phys. Lett. B **13**, 563 (1999)